Accuracy and feasibility of the β^* measurement for LHC and High Luminosity LHC using k modulation

F. Carlier*
CERN, Geneva CH-1211, Switzerland, and NIKHEF, Amsterdam 1098 XG, The Netherlands

R. Tomás
CERN, Geneva CH-1211, Switzerland

(Received 24 February 2016; published 20 January 2017)

The future regimes of operation of the LHC will require improved control of β^* measurements to successfully level the luminosities in the interaction points. The method of k modulation has been widely used in other machines to measure lattice beta functions. In the LHC, k modulation of the closest quadrupoles to the interaction point (IP) is the most accurate method to measure β^* at the IP. This paper highlights the challenge of high precision tune measurements (down to 10^{-5}) for the correct determination of β^* in the high luminosity LHC. Furthermore it presents a new analytical method for the calculation of β^* using k modulation.

DOI: 10.1103/PhysRevAccelBeams.20.011005

I. INTRODUCTION

Betatron functions at the interaction points of the LHC (β^*) must be accurately controlled to maximize luminosity, but also to avoid significant imbalances between the experiments. Future regimes of operations and the upgrade to the high luminosity LHC (HL-LHC) will run at lower β^* and higher luminosities [1]. The luminosity imbalance between the two largest experiments, ATLAS [2] and CMS [3], should not surpass 5% [4,5] and thus dictates an accuracy on β^* measurements of ∼2.5%.

The LHC requires the full commissioning of optics and collimation before any luminosity may be delivered. As such, conventional luminosity tuning methods, such as luminosity scans versus waist would require commissioning of each scan step and cannot be performed within the envisaged commissioning time frame. Accurate methods to determine β^* using single low intensity bunches are therefore important to have good control of the optics at the IP and to provide more accurate luminosity predictions for the experiments.

Currently, the preferred method to calculate β^* in the LHC is based on k modulation of the last quadrupoles before the IP [6,7]. With k modulation, the gradient of a quadrupole is modulated, and the induced tune shifts are measured to determine the average betatron function in that quadrupole. This method has been used successfully to calculate lattice betatron functions in ISR [8,9], LEP [10,11], HERA [12], Tevatron [13], ALBA [14], RHIC [15,16] and more. k modulation was used in LEP to calculate β^* using the method presented in [17]. The LEP symmetric quadrupole layout around the IP made it straightforward to determine the waist shift (w) with respect to the IP, and the equal response from the left and right quadrupoles guaranteed a centered waist. The LHC, however, uses an antisymmetric design of quadrupoles at the IP [18,19] and is the first collider to face the challenges of k modulation for β^* measurement in such a design. In general a nonlinear equation has to be solved to determine w and β^*. Nevertheless we show in this paper that even in antisymmetric designs the waist can be centered by setting the left-right tune response ratio to a certain value given by the optics layout.

The robustness of k modulation to calculate β^* at collision optics ($\beta^* \leq 1.0$ m) is studied and the importance of accurate tune measurements (down to 10^{-5}) is highlighted in this paper. Furthermore, the derivation of a new analytical formula, based on k modulation, to calculate β^* is presented. Both analytical and numerical methods are compared using MAD-X simulations in Sec. VII for the LHC and the HL-LHC. The effect of fringe fields in the triplet quadrupoles has been considered in the MAD-X simulations.

II. k MODULATION

k-modulation studies in this paper are only done for squeezed optics with $\beta^* \leq 1$ m. These squeezed optics will be used for IP1 (ATLAS) and IP5 (CMS) during proton physics runs. IP2 (ALICE) will also reach such small β^* during the heavy ion physics runs. The studies presented here are limited to IP1 for beam 1 for illustration purposes.

Figure 1 shows a sketch of the IP1 setup for the horizontal plane following the conventions used in MAD-X [20] models of the LHC. On the sides are the two quadrupoles closest to the IP on which the modulation will be applied. In the

*felix.simon.carlier@cern.ch

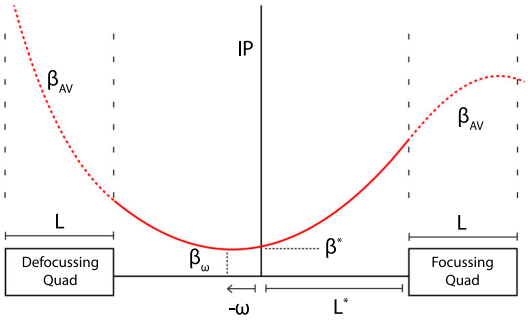

FIG. 1. Schematic representation of interaction region configuration. This corresponds to the default horizontal plane as defined in MAD-X models of the LHC, with a focusing quadrupole on the right and a defocusing quadrupole on the left.

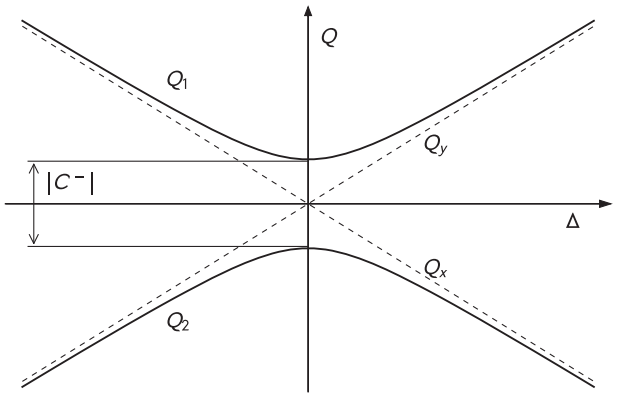

FIG. 2. Schematic representation of the closest tune approach. The unperturbed tunes are labeled as Q_x and Q_y, while the perturbed tunes are given by Q_1 and Q_2.

horizontal plane there is a defocusing quadrupole on the left side and a focusing quadrupole on the right side. The minimum of the β-function in the drift space between the quadrupoles has a value β_w and is located at the waist (w), that is positively defined to the right. The value of the β-function at the IP is given by β^*. Generally β_w is close to β^*, but a shift in w due to optics distortions significantly affects β^*.

The modulation of the quadrupole gradient is applied to both quadrupoles independently and the shifts in the main tunes ($\Delta Q_{x,y}$) are measured separately for each quadrupole. Under good control of linear coupling the amplitude of the modulation at collision tunes ($Q_x = 64.31$ and $Q_y = 59.32$) is generally limited such that

$$\Delta Q^{\text{def}} = \frac{1}{3}(Q_y - Q_x) = 0.0033, \tag{1}$$

where ΔQ^{def} is the tune shift in the defocusing plane of the modulated quadrupole. Exceeding this limit in measurements may drive the main tunes to the coupling stop band.

The closest tune approach in an accelerator is conventionally given by

$$\Delta Q_{\text{min}} = \sqrt{\Delta^2 + |C^-|^2}, \tag{2}$$

where ΔQ_{min} is the tune separation, Δ is the unperturbed tune split, and $|C^-|$ is the magnitude of the linear difference coupling. When the coupling resonance is approached (i.e. $\Delta \to 0$), the minimum tune split is equal to the magnitude of the coupling $|C^-|$, as presented in Fig. 2. The effect of linear coupling on the tune measurements has been studied and is presented in Sec. VII A where tolerances on linear coupling have been specified.

Different tune combinations with larger tune separations, such as the injection tunes for the LHC ($Q_x = 64.28$ and $Q_y = 59.31$), may also be envisaged to mitigate the influence of coupling. Larger tune separations can also allow for larger modulation amplitudes thereby increasing the measurement accuracy. However these will still be limited by enclosing resonances in the tune diagram. Furthermore, drastic changes in tunes will perturb the optics at the interaction points. The studies presented here are done at nominal optics with collision tunes following the typical optics commissioning procedure. All applied modulations in the simulations presented here are limited to Eq. (1).

Modulation of a single quadrupole will induce a measurable tune shift that is proportional to the average betatron function at that quadrupole. Derivations for this relation are presented in [17],

$$\beta_{\text{AV}_{x,y}}(\Delta Q_{x,y}) = \pm[\cot(2\pi Q_{x,y})(1 - \cos(2\pi\Delta Q_{x,y})) + \sin(2\pi\Delta Q_{x,y})]\frac{2}{\Delta K L} \tag{3}$$

$$= \pm 4\pi \frac{\Delta Q_{x,y}}{\Delta K L}, \tag{4}$$

where ΔK is the change of the quadrupole strength, L is the length of the quadrupole, $Q_{x,y}$ and $\Delta Q_{x,y}$ are respectively the main tunes and the tune shifts, and the ($\pm$) sign corresponds to the horizontal and vertical planes. By modulating the last quadrupoles before the IPs independently and measuring the shift in the main tunes, the average β-functions at those quadrupoles can be accurately calculated. To determine w and β^*, $\beta_{\text{AV}_{x,y}}$ should be expressed as a function of the IP parameters. This is presented in the following section.

Second order tune shifts arising from tilts in the modulated quadrupoles can however perturb the tune measurements during the modulations. Tilts in quadrupoles give rise to skew quadrupolar field components proportional to the quadrupole powering strength. The second order tune shifts arising from skew quadrupolar contributions have been studied in [21] and are given by two sums over all skew quadrupolar sources ($\mathbf{j}$, $\mathbf{k}$):

$$\Delta Q_{x,y} = \frac{1}{16\pi}\sum_j \sum_k (a_{1j} a_{1k} \sqrt{\beta_{xj}\beta_{xk}\beta_{yj}\beta_{yk}}(\pm T^{1-1}_{jk} - T^{11}_{jk})), \tag{5}$$

where the plus or minus sign refers to the horizontal and vertical planes respectively, a_{1j} and a_{1k} are the field strength components, and where $T_{\mathbf{jk}}$ is defined as

$$T^{\mathbf{n}}_{\mathbf{jk}} \equiv \frac{\cos[\mathbf{n}\cdot(\phi^{+}_{\mathbf{jk}} - \boldsymbol{\mu}/\mathbf{2})]}{\sin[\mathbf{n}\cdot\boldsymbol{\mu}/\mathbf{2}]}, \tag{6}$$

where $\boldsymbol{\mu}$ are the main tunes, $\mathbf{n}$ is either the difference or sum resonance in the case of skew quadrupolar contributions and $\phi^{+}_{\mathbf{jk}}$ is the phase advance between the different skew quadrupolar sources in the accelerator and specified as

$$\phi^{+}_{\mathbf{jk}} = \begin{cases} \phi_{\mathbf{k}} - \phi_{\mathbf{j}}, & j < k \\ \phi_{\mathbf{j}} - \phi_{\mathbf{k}}, & k < j. \end{cases} \tag{7}$$

The second order tune shifts may be viewed as the parabolic approximation of Fig. 2 and will generally be dominated by the difference resonance in both the LHC and HL-LHC. The HL-LHC is expected to have rms tilts of 1 mrad in the triplet quadrupoles [22]. The effect of such tilts has been studied and is presented in Sec. VII.

III. AVERAGE β-FUNCTION IN QUADRUPOLES

The propagation of the Twiss parameters in quadrupoles [17,23,24] is given by

$$\begin{pmatrix} \beta(s) \\ \alpha(s) \\ \gamma(s) \end{pmatrix} = \begin{pmatrix} C^2 & -2CS & S^2 \\ -CC' & SC' + S'C & -SS' \\ C'^2 & -2S'C' & S'^2 \end{pmatrix} = \begin{pmatrix} \beta_0 \\ \alpha_0 \\ \gamma_0 \end{pmatrix}. \tag{8}$$

The parameters C and S for a focusing quadrupole are the sinelike functions given by $C = \cos(\sqrt{K}s)$ and $S = \frac{1}{\sqrt{K}}\sin(\sqrt{K}s)$. Here, K is the quadrupole gradient and s is the longitudinal position within the quadrupole. Note that in the case of the defocusing plane of the quadrupoles Eq. (8) is composed of hyperbolic functions such that $S = \frac{1}{\sqrt{K}}\sinh(\sqrt{K}L)$ and $C = \cosh(\sqrt{K}L)$. For illustration purposes, the following derivations only use focusing quadrupoles. The results for defocusing quadrupoles will be given at the end. The propagation of the β-function is calculated from Eq. (8) and the average β-function is calculated by integrating the β-function over the length of the quadrupole L and normalizing by the same length L, which yields

$$\beta^{\mathrm{foc}}_{\mathrm{AV}} = \frac{\beta_0}{2}\left(1 + \frac{\sin(2\sqrt{K}L)}{2\sqrt{K}L}\right) - \alpha_0\frac{\sin^2(\sqrt{K}L)}{\sqrt{K}L\cdot\sqrt{K}} + \frac{\gamma_0}{2K}\left(1 - \frac{\sin(2\sqrt{K}L)}{2\sqrt{K}L}\right), \tag{9}$$

where $\beta^{\mathrm{foc}}_{\mathrm{AV}}$ is the average β-function in the focusing quadrupole. The average β function is only dependent on design machine parameters (K, L) and optics parameters at the beginning of the quadrupole (α_0, β_0, γ_0). These optics parameters can be calculated by propagation from the IP, Eq. (10), and be used to find an expression for $\beta^{\mathrm{foc}}_{\mathrm{AV}}$ that depends on β_w and waist (w):

$$\begin{aligned} \beta_0 &= \beta_w + \frac{(L^* - w)^2}{\beta_w} \\ \alpha_0 &= -\frac{1}{2}\beta' = -\frac{(L^* - w)}{\beta_w} \\ \gamma_o &= \frac{1 + \alpha_0^2}{\beta_0} = \frac{1}{\beta_w}, \end{aligned} \tag{10}$$

where the distance between the IP and the first quadrupole is given by L^*. The expression for the average β-function in focusing quadrupoles is then given by

$$\beta^{\mathrm{foc}}_{\mathrm{AV}} = \frac{1}{2}\left[\beta_w + \frac{(L^* - w)^2}{\beta_w}\right]\left(1 + \frac{\sin(2\sqrt{K}L)}{2\sqrt{K}L}\right) + \frac{(L^* - w)}{\beta_w}\frac{\sin^2(\sqrt{K}L)}{\sqrt{K}L\cdot\sqrt{K}} + \frac{1}{2\beta_w K}\left(1 - \frac{\sin(2\sqrt{K}L)}{2\sqrt{K}L}\right). \tag{11}$$

A convenient assumption can be made to simplify this equation. Assuming that $\beta^* \ll L^*$ and $|w| \ll L^*$, the following can be stated:

$$\frac{(L^* \pm w)^2}{\beta_w^2} \gg 1. \tag{12}$$

This approximation is only valid for squeezed optics and therefore limits the studies done in this paper to $\beta^* \leq 1$ m in the LHC and HL-LHC. For the purpose of readability the following functions are defined:

$$\begin{aligned} f_0 &= \frac{1}{2}\left(1 + \frac{\sin(2\sqrt{K}L)}{2\sqrt{K}L}\right), \\ f_1 &= \frac{\sin^2(\sqrt{K}L)}{\sqrt{K}L\cdot\sqrt{K}}, \\ f_2 &= \frac{1}{2K}\left(1 - \frac{\sin(2\sqrt{K}L)}{2\sqrt{K}L}\right), \\ d_0 &= \frac{1}{2}\left(1 + \frac{\sinh(2\sqrt{K}L)}{2\sqrt{K}L}\right), \\ d_1 &= \frac{\sinh^2(\sqrt{K}L)}{\sqrt{K}L\cdot\sqrt{K}}, \\ d_2 &= \frac{1}{2K}\left(\frac{\sinh(2\sqrt{K}L)}{2\sqrt{K}L} - 1\right). \end{aligned}$$

Using these new expressions and the approximation in Eq. (12) the average β-function in the focusing and defocusing quadrupoles is given by

$$\beta_{\mathrm{AV}}^{\mathrm{foc}} = \frac{(L^* - w)^2}{\beta_w} f_0 + \frac{(L^* - w)}{\beta_w} f_1 + \frac{1}{\beta_w} f_2 \quad (13)$$

$$\beta_{\mathrm{AV}}^{\mathrm{def}} = \frac{(L^* + w)^2}{\beta_w} d_0 + \frac{(L^* + w)}{\beta_w} d_1 + \frac{1}{\beta_w} d_2. \quad (14)$$

IV. ANALYTICAL METHOD FOR β^* CALCULATION

Previous β^* calculations using k modulation in the LHC were based on numerically solving an equation dependent on ΔQ_R and ΔQ_L (for the quadrupoles left and right of the IP) where the coefficients were determined from simulations [6]. The derivation of a closed formula based on k modulation to calculate β^* is presented in this section. The ratio between the average β-functions in the defocusing and focusing quadrupoles left and right of the IP, χ, is defined as follows:

$$\chi = \frac{\beta_{AV}^{\mathrm{def}}}{\beta_{AV}^{\mathrm{foc}}}. \quad (15)$$

The values of the average β-functions can be calculated from the measured tune shifts obtained from k modulation using Eq. (3). The tune shifts are constrained such that the tune shifts generated by the left and right quadrupoles must have the same sign. This corresponds to a symmetric quadrupole modulation where the ΔK on the left and right quadrupoles has the same sign.

Using Eqs. (13) and (14) for the average β-function, an expression for χ is obtained that is only dependent on machine parameters and the waist (w):

$$\chi(w) = \frac{(L^* + w)^2 d_0 + (L^* + w) d_1 + d_2}{(L^* - w)^2 f_0 + (L^* - w) f_1 + f_2}.$$

Interestingly, the ratio χ for which the waist is aligned at the IP ($w = 0$) only depends on model parameters,

$$\chi(0) = \frac{L^{*^2} d_0 + L^* d_1 + d_2}{L^{*^2} f_0 + L^* f_1 + f_2}. \quad (16)$$

Assuming that $\sqrt{K}L$ is small, the sinelike terms can be expanded. Refactoring the terms yields the following approximation:

$$\chi(0) \approx \frac{3 + KL^2}{3 - KL^2}. \quad (17)$$

This gives a very quick and practical approximation to calculate χ for which the waist is zero. It is found that the waist is zero in the LHC and HL-LHC when

$$\chi_{\mathrm{LHC}} = 1.264 \approx 1.267$$
$$\chi_{\mathrm{HL-LHC}} = 1.283 \approx 1.288,$$

where the first value is obtained using the exact formula in Eq. (16) and the second value is obtained using the approximation of Eq. (17). Note that for colliders with symmetric triplet designs, such as for LEP, the ratio becomes one, $\chi = 1$. The following procedure may be proposed to set the waist to zero before calculating β^*. First, the average β-functions in the quadrupoles are measured. The waist is then varied using the matching section quadrupoles until the right ratio (χ) of β-functions is found, at which point the waist is zero. k modulation of the quadrupoles can then be done to calculate β^*. It is shown in Sec. VI that the best β^* resolution is indeed obtained for $w = 0$.

Reformatting Eq. (16) yields the following second order polynomial for the waist:

$$(\chi f_0 - d_0) w^2 - [2L^*(\chi f_0 + d_0) + (\chi f_1 + d_1)] w + L^{*^2}(\chi f_0 - d_0) + L^*(\chi f_1 - d_1) + (\chi f_2 - d_2) = 0. \quad (18)$$

Equation (18) can be solved for w for which the real part of the solution is used to obtain

$$w = \frac{1}{2(\chi f_0 - d_0)} [[2L^*(\chi f_0 + d_0) + (\chi f_1 d_1)] \pm [16L^{*^2}\chi f_0 d_0 + 8L^*(\chi f_1 d_0 + \chi f_0 d_1) + (\chi f_1 + d_1)^2 - 4(\chi f_0 - d_0)(\chi f_2 - d_2)]^{1/2}]. \quad (19)$$

Combining Eq. (3) with Eqs. (13) and (14) it is now possible to calculate β_w from the β_{AV} of the two quadrupoles:

$$\beta_w^{\mathrm{foc}} = \frac{1}{\beta_{AV}^{\mathrm{foc}}} \cdot [(L^* - w)^2 f_0 + (L^* - w) f_1 + f_2]$$
$$\beta_w^{\mathrm{def}} = \frac{1}{\beta_{AV}^{\mathrm{def}}} \cdot [(L^* + w)^2 d_0 + (L^* + w) d_1 + d_2]. \quad (20)$$

Both equations yield the same betatron function at the waist. To account for small deviations or numerical fluctuations the average of the two is taken, $\beta_w = \frac{1}{2}(\beta_w^{\mathrm{foc}} + \beta_w^{\mathrm{def}})$. Using this, the final result for β^* can be calculated using the drift space Eq. (21):

$$\beta^* = \beta_w + \frac{w^2}{\beta_w}. \quad (21)$$

Note that the derivation of this method is fully analytical and that the only approximation is made in Eq. (12). It

should therefore be stated that this method is limited to small IP β-functions ($\beta^* \leq 1$ m).

V. FRINGE FIELDS

Usually, the magnetic fields at the edges of magnets are modeled as a step function. However, such a representation is unrealistic and the field decays smoothly. The transitional area of the magnetic field at the edge of the magnet is called the fringe field. As the quadrupoles are located in a large β-function region, any imperfection such as fringe fields may impact the transverse beam size at the IPs. Furthermore, quadrupole fringe fields affect the ring optics and consequently the tune shifts resulting from k modulation and may therefore affect the measurements of w and β^* using current methods.

Fringe fields have been included in the simulation to provide deeper insight in the applicability of k modulation to the measurements of the IP optics. The linear fringe fields shape can be modeled using the fifth order Enge function [25],

$$F(z) = \frac{1}{1 + \exp\left[a_0 + a_1\left(\frac{z}{D}\right) + \cdots + a_5\left(\frac{z}{D}\right)^5\right]}, \tag{22}$$

where the parameters $\{a_0 \cdots a_5\}$ are obtained from fits to simulated values of the field gradient [26], z is the position with respect to the magnet hard edge, and D is the aperture of the magnet. The resulting fringe field strength is obtained by

$$K_{\mathrm{fr}}(z) = K_{\mathrm{quad}} F(z). \tag{23}$$

Fringe-field simulations were done for the MQXF quadrupoles planned to be used in the HL-LHC. Unfortunately, such simulations are not available for the MQXA quadrupoles currently installed in the LHC. The parameters $\{a_0 \cdots a_5\}$ are assumed to be unchanged for the two magnets, and the magnetic profile for the MQXA magnets are obtained by scaling the aperture D from $D = 150$ mm to $D = 70$ mm.

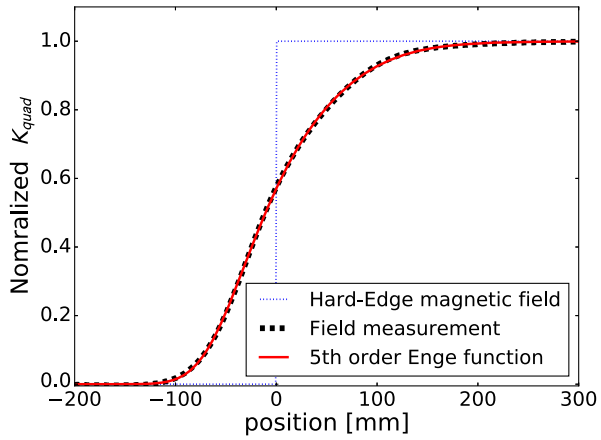

FIG. 3. Fringe field as simulated [26] and modeled for the MQXF quadrupoles with an aperture of 150 mm. In black is the simulated field of the magnet, and in red is the modeled field using the fifth order Enge function. The modeled fringe field agrees very well with the simulated data and validates the used order of the Enge function.

TABLE I. Parameters for the fifth order Enge function obtained from a fit to the magnetic profile of the MQXF quadrupoles.

Parameter	Fit value
a_0	−0.2829102
a_1	−3.83589587
a_2	1.94849646
a_3	−2.69675443
a_4	1.288764
a_5	−0.18566207

Figure 3 shows the fifth order Enge function fit to the MQXF magnetic profile [26]. The obtained parameters are given in Table I.

A. Modeling fringe fields

For the studies done here, fringe fields were modeled in MAD-X. The fringe field shape is defined by the Enge function in Eq. (22), and the fit parameters were obtained to fit the simulated data of the MQXF magnets. The fringe field starts 20 cm before the quadrupole and ends 30 cm inside the quadrupole, for both the MQXF and MQXA magnets in the HL-LHC and LHC, respectively. In MAD-X the fringes on both sides of the magnets are sliced up into 100 elements whose quadrupole strengths are obtained by the Enge function. The integrated quadrupole strength conserved by rescaling the gradient K after applying fringe fields,

$$KL|_{\mathrm{w/o\,fringes}} = \int_L K(s)\mathrm{d}s|_{\mathrm{incl\ fringes}}. \tag{24}$$

The fringe fields are only modeled for the last quadrupoles of the IR1 triplets, therefore reducing the global effect on the β-function around the ring. Including fringe fields in the model induces a shift in the main tunes due to the change of the magnetic profile of the triplet quadrupoles. As β^* decreases the β-function in the triplets increases thereby increasing the expected effect of fringe fields on the optics and hence on the tune shifts [27].

VI. MEASUREMENT UNCERTAINTY IN β^* USING k MODULATION

This section presents the study done to show the effect of accuracy in tune measurements on the uncertainty of β^* measurements using k modulation. It highlights the importance of accurately measuring the tune up to $\delta Q \pm 10^{-5}$. It

should be noted that the recent studies predict a poorer tune stability for the HL-LHC, up to $\delta Q \pm 10^{-4}$ [28,29].

A dedicated computer code in PYTHON has been made to calculate the resulting uncertainties on the calculated waist and β^* from the tune shifts, $\Delta Q_{x,y}$. The setup is based on the horizontal plane of IP1 for beam 1, as presented in Sec. II. A domain is initialized for different values of waist (w) and β_w with the following limits:

$$\beta_w \in [0.8 \cdot \beta^*_{\text{design}}, 1.2 \cdot \beta^*_{\text{design}}]$$
$$w = \left[-\frac{1}{2}\beta^*_{\text{design}}, \frac{1}{2}\beta^*_{\text{design}}\right],$$

where for the LHC, $\beta^*_{\text{design}} = 0.55$ m, and for the HL-LHC, $\beta^*_{\text{design}} = 0.15$ m. For each β_w and waist in the specified domain, the β-functions at the IP and at the edge of the quadrupoles left and right of the IP are calculated. Using the Twiss parameters at the edge of each quadrupole, the average β-function can be calculated using Eq. (11) for the focusing quadrupole on the right and appropriate equivalent for the defocusing quadrupole on the left. The tune shifts $\Delta Q_{x,y}$ can then be determined using the approximation in Eq. (4), where ΔK is obtained from Eq. (1) at collision tunes. Note that the approximation of Eq. (4) is used in this case for the purpose of increasing the computational speed.

For each point in this measured domain, the uncertainty on β^* can be calculated by searching through the neighboring points fulfilling the condition $\Delta Q^{\text{foc}} \pm 10^{-5}$ and $\Delta Q^{\text{def}} \pm 10^{-5}$. The spread in β^* of the neighboring points satisfying this condition is a measure of the uncertainty on β^* measurements.

Figure 4 shows the relative uncertainty on the β^* measurement ($\Delta\beta^*/\beta^*$) for a tune resolution of 10^{-5} for the LHC in the top figure, while the bottom figure shows the same analysis for the HL-LHC. The uncertainty for the LHC is minimal (0.5%) for $w = 0$, and grows with increasing waist deviation. The HL-LHC has a minimum uncertainty of 4% and the uncertainty grows more rapidly for increasing waist. Figure 4 clearly shows that for the same relative waist deviation $\frac{w}{\beta^*_{\text{design}}}$, the HL-LHC will have a much larger uncertainty. It will therefore be crucial to have good control of the waist, probably assuming an iterative

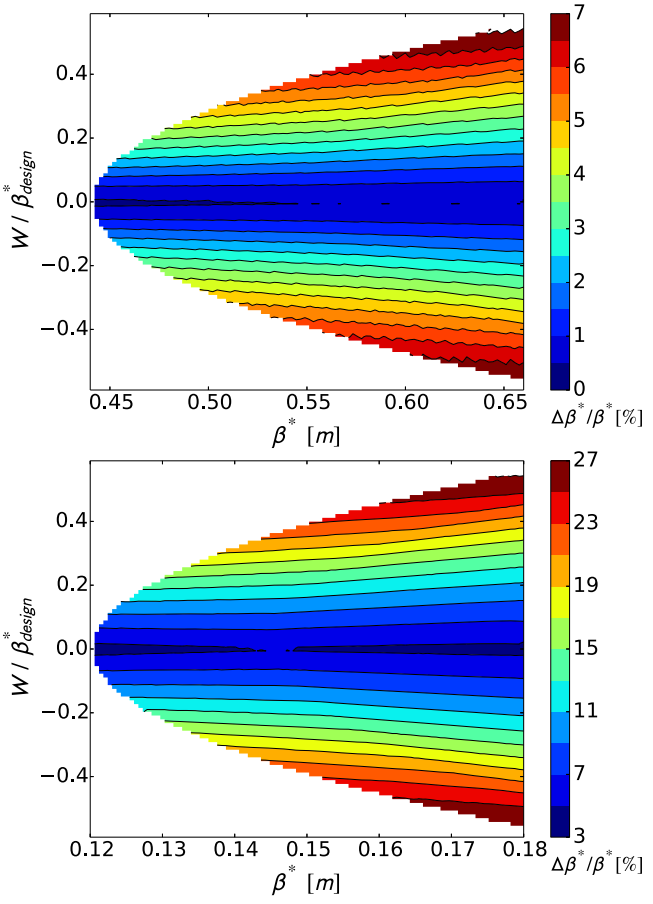

FIG. 4. Uncertainty on β^* measurements for $\delta Q \pm 10^{-5}$ using k modulation for the LHC (top figure) and HL-LHC (bottom figure). The vertical axis shows the waist relative to the design β^* (LHC: $\beta^*_{\text{design}} = 0.55$ m, HL-LHC:$\beta^*_{\text{design}} = 0.15$ m).

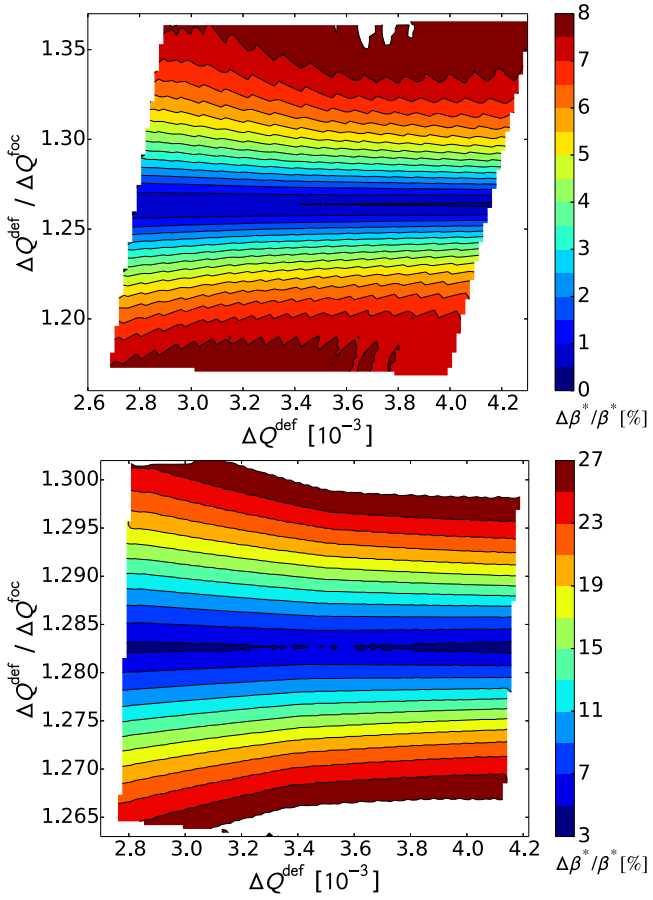

FIG. 5. Uncertainty $\Delta\beta^*/\beta^*$ for the LHC (top figure) and HL-LHC (bottom figure) over the relevant tune shifts. The minimum error occurs at $\chi(0)$ for both the LHC and HL-LHC.

procedure, to reach the minimal uncertainty at $w = 0$, as discussed in Sec. IV.

The calculated uncertainty on β^* for a tune resolution of $\delta Q = 10^{-5}$ is shown in Fig. 5 versus the measured tune shifts, for both the LHC and HL-LHC. The values of the ratio $\chi \approx \frac{\Delta Q^{\mathrm{def}}}{\Delta Q^{\mathrm{foc}}}$ for which the uncertainty is minimal correspond to those calculated in Eq. (16) for $w = 0$. The range of $\frac{\Delta Q^{\mathrm{def}}}{\Delta Q^{\mathrm{foc}}}$ on the vertical axis is much smaller for the HL-LHC indicating that the β^* measurements for the HL-LHC are much more sensitive to the tune measurement precision of $\delta Q \pm 10^{-5}$.

These results indicate that, while accurate measurements of β^* for the LHC are possible at $\beta^* = 0.55$ m, the accuracy of β^* measurements for the HL-LHC degrades significantly. This highlights the great challenge of accurately measuring and controlling β^* for the HL-LHC.

VII. CALCULATION OF β^* IN MAD-X SIMULATIONS

The results presented in this section are obtained from MAD-X simulations using beam 1 at IP1. The MAD-X simulations were run by changing the quadrupole gradient, and measuring the tune shifts for both planes. From these tune shifts β^* was calculated using the analytical method.

The studies presented here are done using a positive modulation of the quadrupole gradient. Results obtained using a negative gradient are similar to these presented here. Furthermore, these simulations were done with fringe fields modeled at the quadrupoles. Results are only shown for the horizontal plane only, but are also illustrative for the vertical plane.

Figure 6 compares the deviation of the calculated β^* to the design optics obtained from the analytical method for both the LHC and HL-LHC. The analytical method accurately calculates the IP β-functions for the different optics. The maximum deviation, at $\beta^* = 1$ m for the LHC, to the design optics is small (within 0.21%) and the calculated β^* converges to the design optics value for smaller β^*. The larger deviation observed for increasing β^* is attributed to the approximation made in Eq. (12). Furthermore, a small additional deviation of 0.07% is observed throughout the complete range of IP sizes. This deviation is caused by the implementation of the fringe fields in the quadrupoles. Triplet fringe fields will induce a shift in the waist that will in turn increase the β-functions at the IPs.

The uncertainty for the analytical method is determined by calculating β^* for the domain that satisfies $\Delta Q^{\mathrm{def}} \pm 10^{-5}$ and $\Delta Q^{\mathrm{foc}} \pm 10^{-5}$ and determining the spread, $\frac{1}{2}(\beta^*_{\mathrm{max}} - \beta^*_{\mathrm{min}})$. The standard deviation grows rapidly for decreasing β^*. The uncertainty at $\beta^* = 0.55$ m is 0.5% which is slightly larger than the results obtained in the simulations of Sec. VI, which can be attributed to the fringe

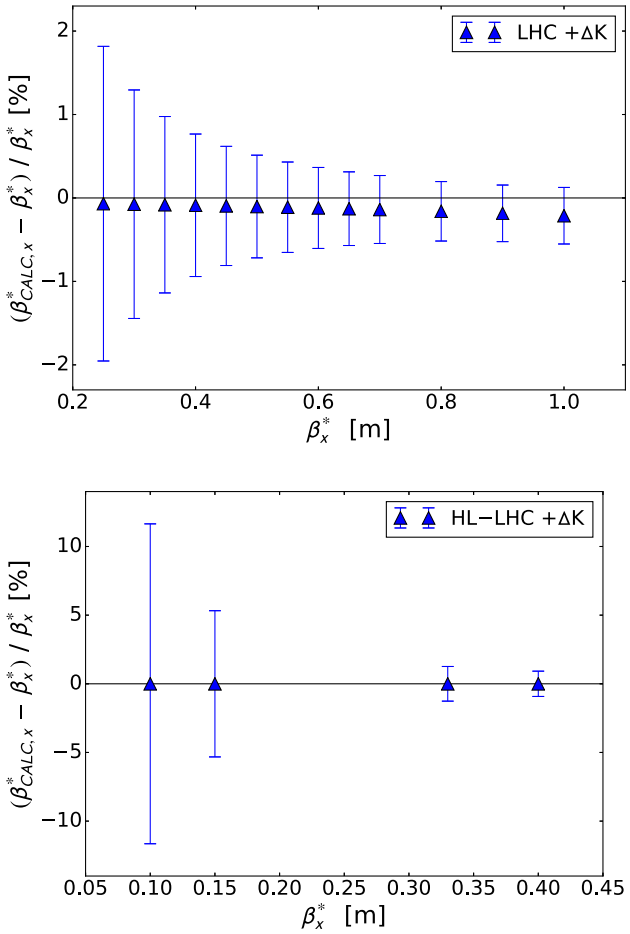

FIG. 6. The calculated β^* calc using the new analytical method in the LHC (top figure) and HL-LHC (bottom figure) including the effect of fringe fields on the last quadrupoles. Results are presented for the horizontal plane.

fields in the MAD-X simulations. Recent k-modulation measurements at $\beta^* = 0.8$ m are demonstrating a tune resolution close to $\delta Q = 10^{-5}$ and a resolution on β^* that is lower than 1% [30,31]. These results are in line with the predictions from the simulations.

The previous analysis is also presented for the HL-LHC in Fig. 6. Fewer optics are available but the general behavior observed for the LHC can be confirmed in the HL-LHC. The deviation measured for the range of optics in HL-LHC is negligibly small. However, Fig. 6 shows the degrading accuracy for decreasing β^*. Measurements for the design optics of the HL-LHC at $\beta^* = 0.15$ m show an error of 5.2% arising from a tune resolution of $\delta Q = 10^{-5}$. Such large uncertainties for small β^* will create a considerable challenge for accurate β^* control for the HL-LHC.

These results show that the analytical method can be used to measure low β^* optics, and provides a robust way to calculate measurement errors. The calculation of the measurement errors can easily be extended to include other possible sources of uncertainty. As such, the finite accuracy of the quadrupole gradient (δK) as well as alignment of the

quadrupoles (δL^*) can now be included. The following values have been used for the analysis; $\delta K \pm 0.1\%$ and $\delta L^* \pm 6$ mm. Such misalignment errors have been estimated in [32] and have been shown to be mechanically achievable.

Figure 7 shows the errors obtained from various sources for the LHC and HL-LHC respectively. In red are the calculated errors for simulations without fringe fields. In blue are the obtained errors when including the fringe fields in the simulations. These are the same as shown in Fig. 6. The implementation of fringe fields slightly increases the calculated errors on β^*. This effect is, however, only limited to 0.2% for the LHC and 1% for the HL-LHC in the smallest optics.

The data in green shows the errors when including contributions from the quadrupole powering (δK) and possible misalignments of the quadrupoles (δL^*). Including these new sources significantly increases the errors on β^* measurements. In the LHC the error for the smallest optics is increased by 0.6%, while in the HL-LHC the error is increased by 4% at $\beta^* = 0.10$ m. This effect becomes non-negligible for decreasing β^* sizes and further confirms that such contributions as accuracy of the transfer function and alignments should therefore be considered in the analysis to improve β^* control.

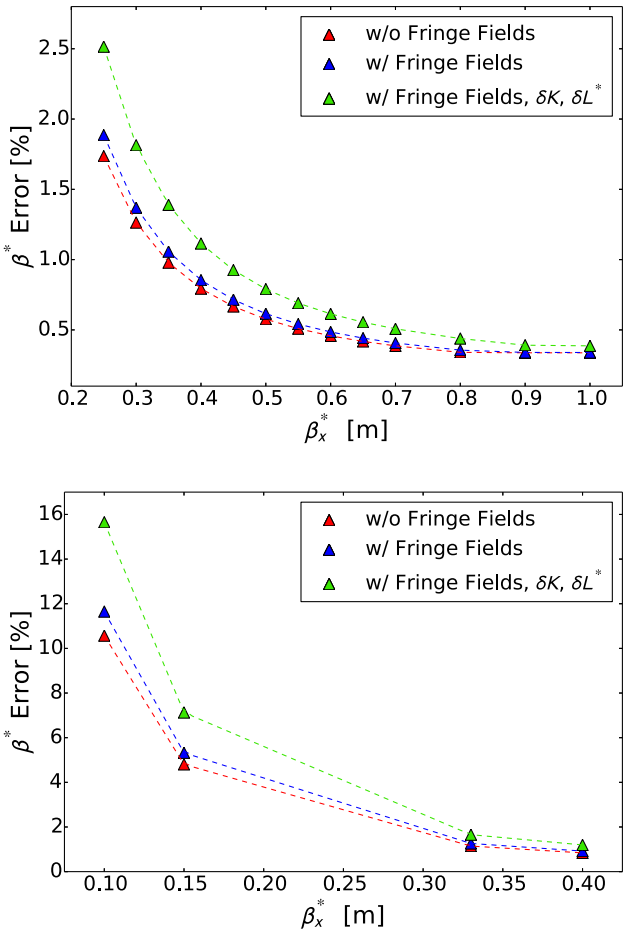

FIG. 7. Calculated errors using the analytical method for different contributions and for the range of LHC (top figure) and HL-LHC (bottom figure) optics. In red are the errors found for simulations without fringe fields. Results as presented before are shown when including fringe fields are shown in blue, while errors found when including uncertainties in K (0.1%) and L^* (6 mm) are shown in green.

In addition to these sources, recent studies have shown that the tune stability for the HL-LHC will not be as good as for the LHC. Tune stability is estimated to be between 5×10^{-5} and 10^{-4} [28,29]. These estimates may be subject to changes as powering schemes for the quadrupoles are being revisited. The influence of the tune uncertainty on the β^* resolution is shown in Fig. 8 for different optics. The results show that only the larger β^* optics, 0.33 and 0.40 m, currently result in reasonable β^* resolution for $\delta Q \leq 2 \times 10^{-5}$. The current design optics for the HL-LHC does not satisfy machine requirements. For a tune resolution of 5×10^{-5} the design optics at 0.15 m will have a error of 120% on β^*. This clearly shows that a degrading tune stability will critically spoil the accuracy of β^* measurements using k modulation. The accuracy can be improved by increasing the tune separation and using larger modulation amplitudes. However, such gains are limited to a few factors and do not account for 2 orders of magnitude. As such, this motivates further development of the k-modulation method, and has motivated the search for alternative methods to calculate β^* such as the use of ballistic optics to calibrate beam position monitors (BPMs) in order to accurately measure β-functions from oscillation amplitudes [33].

A. Influence of linear coupling and quadrupole tilts

Simulations have been performed in MAD-X to study the influence of both linear coupling and tilts in triplet quadrupoles on the tune measurements and accuracy of β^* calculations. A pessimistic approach has been used, in which a positive modulation is applied thereby increasing

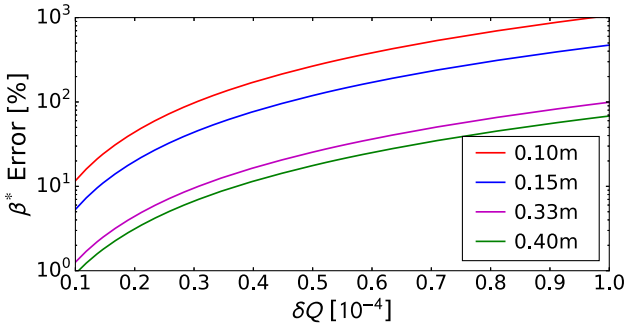

FIG. 8. Error on β^* measurements versus the tune accuracy for different optics. The error grows rapidly with increasing tune uncertainty. A tune resolution of 5×10^{-5} will result in an 120% error on the β^* measurement for the design optics of $\beta^* = 0.15$ m.

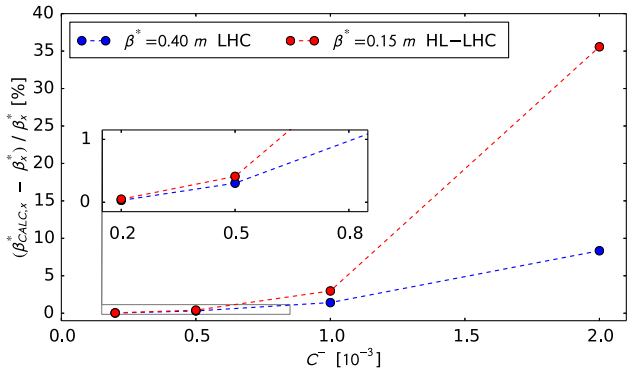

FIG. 9. Deviation of calculated β^* for different values of coupling for the LHC (top figure) and HL-LHC (bottom figure). Results show an increased deviation for increasing coupling in the accelerator.

quadrupole strength and thus causing the main tunes to approach each other. A negative modulation will cause the tunes to move apart and thus minimize the effect of coupling. However, as current methods include sinusoidal modulations of the quadrupoles the pessimistic case cannot be neglected [7,34].

Figure 9 shows the resulting β^* deviation for different values of coupling for nominal optics in the LHC and HL-LHC. The deviation of β^* to the model increases as the coupling is increased and at $|C^-| = 2 \times 10^{-3}$ reaches 8.3% for the LHC optics at 0.40 m and up to 36% for the 0.15 m optics in the HL-LHC.

To keep the effect of coupling on β^* accuracy lower than 1%, coupling should be corrected to $|C^-| \leq 8 \times 10^{-4}$ for the LHC and down to 6×10^{-4} for the HL-LHC. Though challenging, it has been recently shown that accurate coupling corrections, down to $|C^-| = 2 \times 10^{-4}$, can be achieved in the LHC [35]. The obtained results for the LHC as well as simulation results for coupling corrections presented in [22] indicate that the set tolerance for the HL-LHC is within reach.

Tilts in the IR triplets have been studied by applying 1 mrad rotations to both quadrupoles left and right of the IP

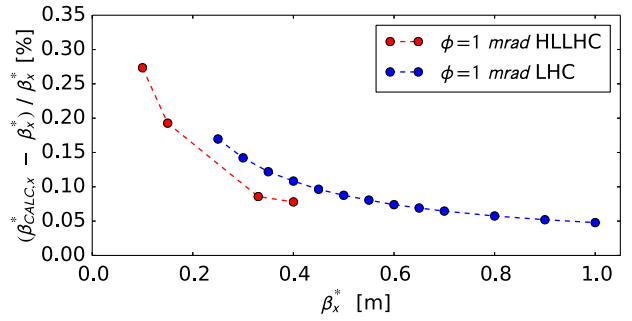

FIG. 10. Deviations of calculated β^* for the different optics of the LHC and HL-LHC, independently showing the effect of linear coupling with $C^- = 5 \times 10^{-4}$ and a quadrupole tilt of 1 mrad. Though the effect is small for both, a quadratic increase of the deviations for decreasing β^* is observed.

and determine the deviation of the calculated β^* to the model. The introduced coupling from the quadrupole tilts has been rematched in the machine to study the effect of tilts independently of coupling. Figure 10 shows the β^* deviation obtained from simulations for both the LHC and HL-LHC at different optics with a 1 mrad tilt. As expected from Eq. (5) the deviation increases rapidly with decreasing β^*. Tilts of 1 mrad in the modulated quadrupoles have a small influence on the accuracy of β^* measurements, and deviations do not exceed 0.29% in both the LHC and HL-LHC. The contribution of quadrupole tilts to β^* errors can be neglected for the currently envisaged optics in both accelerators.

VIII. CONCLUSIONS

k modulation of the last quadrupoles of the IP triplets is currently the preferred method to measure β^*. The accuracy of this method is mainly determined by the precision of the tune measurements. The studies done highlight the importance of precise tune measurements (down to 10^{-5}) for the low β^* regimes. All studies presented here make use of a tune accuracy of 10^{-5}. However, more recent design studies for the HL-LHC predict a tune stability of the order of 5×10^{-5}. Results presented for the HL-LHC are therefore optimistic.

A closed formula was successfully derived to calculate the waist and β^* in an asymmetric IP design. This formulation provides a new method to set the waist to zero. The analytic formulation shows that the waist is zero when the ratio of the average β-functions (χ) of the quadrupoles left and right of the IP is equal to a specific value that only depends on machine settings. When the ratio is set to $\chi_{\mathrm{LHC}} = 1.264$, for the LHC, and $\chi_{\mathrm{HL-LHC}} = 1.283$, for the HL-LHC, the waist is at zero.

A new procedure is proposed to align the waist and calculate β^*. First the average β-functions in the quadrupoles are measured using k modulation. The waist is varied until the specific ratio χ is reached, at which point the waist is zero which provides the best accuracy for β^* measurements. Following that, β^* can be calculated using k modulation and the analytical formula. This method provides a new way to set the waist to zero and calculate β^* and improves the control over asymmetric IP optics in colliders.

The simulations done in Sec. VI clearly show the effect of the waist variation on the accuracy of β^* measurements. For zero waist the uncertainty on β^* for the LHC is 0.4% and 4% for the HL-LHC. Small changes in the waist can significantly impact the uncertainty in β^* measurements. For the LHC, a 20% relative waist deviation ($w/\beta_{\mathrm{design}}$) results in a 3.5% uncertainty on β^* measurements. However, in the case of the HL-LHC a 20% relative waist deviation leads to a 13% uncertainty on β^*. This clearly highlights the sensitivity to the waist and the need for carefully aligning the minimum β-function at the IP to reduce the waist.

k-modulation simulations were done in MAD-X with modeled fringe fields for a range of IP sizes. The fringe fields in the last quadrupoles of the triplets have little effect on the β^* measurements using k modulation. The calculated β^* deviates by 0.1% when including the fringe fields and the uncertainty on β^* increases by 0.2% and 1% for the smallest optics for the LHC and HL-LHC, respectively. The analytical formula provides a robust way to calculate measurement errors as well as systematic errors.

The measurement error calculated for the LHC at design optics ($\beta^* = 0.55$ m) is 0.5%, and grows to 1.9% for $\beta^* = 0.25$ m. This is still within machine requirements. However, the errors found for the HL-LHC are much larger. For the design optics with $\beta^* = 0.15$ m, the errors are 5.2%, and this grows to 12% for $\beta^* = 0.10$ m.

The error analysis can be further expanded using the analytical method to include sources such as uncertainty of quadrupole powering and possible misalignments. The effect of a quadrupole gradient error of 0.1% and a longitudinal alignment uncertainty of 6 mm for the quadrupoles was investigated. Including these errors has a significant impact on the uncertainty of β^* measurements where the uncertainty is increased to 2.5% for the LHC at $\beta^* = 0.25$ m and 16% for the HL-LHC at $\beta^* = 0.10$ m. This further highlights the challenge of using k modulation to calculate the IP optics in the HL-LHC.

These results show that accurate tune measurements (down to 10^{-5}) are sufficient for the LHC, and that such accuracy is crucial and mandatory in the case of the HL-LHC. Recent predictions estimate the tune stability of the HL-LHC to be between 5×10^{-5} and 10^{-4}. The resolution on β^* measurements in the HL-LHC grows rapidly with degrading tune stability, which poses a clear challenge to correctly measure and control IP optics in the HL-LHC. The accuracy of β^* measurements for the design optics of 0.15 m will be 120%. This clearly motivates further development of the k-modulation method and the search for possible alternative methods to calculate the IP optics.

The effect of linear coupling and quadrupole tilts has been studied for both the LHC and HL-LHC. The simulations results show that accurate coupling measurements and corrections will be crucial for the HL-LHC, and a coupling tolerance of $|C^-| \leq 6 \times 10^{-4}$ will be necessary to minimize the effect of coupling to less than 1% in the HL-LHC. Furthermore, results obtained from simulations with 1 mrad tilts in the modulated quadrupoles show that the effect on β^* calculations are limited to 0.18% for $\beta^* = 0.25$ m in the LHC, and 0.29% for $\beta^* = 0.10$ m in the HL-LHC. As such, these results show that quadrupolar tilts up to 1 mrad do not play a large role in the k-modulation measurements for both accelerators.

To conclude, the current status of the k-modulation method is sufficient to control β^* up to 1% in the LHC optics. However, current predictions show that the accuracy of k modulation will be insufficient for the HL-LHC for the estimated tune stability. A combined effort on improving the triplet power supply jitter, the accuracy of the tune measurement, and exploring working points with larger tune spreads will be needed to overcome the presented challenges and allow the use of k modulation at $\beta^* \leq 0.15$ m.

ACKNOWLEDGMENTS

Particular thanks go to Gianluigi Arduini and Massimo Giovannozzi for proofreading the manuscript and providing useful and valuable insights.

[1] HL-LHC Preliminary Design Report: Deliverable: D1.5, Technical Report, 2014.
[2] ATLAS Collaboration homepage, http://atlas.web.cern.ch/Atlas/Collaboration/.
[3] CMS Collaboration homepage, http://cms.web.cern.ch/.
[4] R. Tomas, T. Bach, R. Calaga, A. Langner, Y. I. Levinsen, E. H. Maclean, T. H. B. Persson, P. K. Skowronski, M. Strzelczyk, G. Vanbavinckhove, and R. Miyamoto, Phys. Rev. ST Accel. Beams **15**, 091001 (2012).
[5] E. Meschi, ATLAS and CMS luminosity, LHC Machine Committee meeting, 2012.
[6] R. Calaga, R. Miyamoto, R. Tomas, and G. Vanbavinckhove, Beta* measurement in the LHC based on K modulation, Technical Report No. CERN-ATS-2011-149, 2011.
[7] M. Kuhn, B. Dehning, V. Kain, R. Tomas, G. Trad, and R. Steinhagen, New tools for K modulation in the LHC, Technical Report No. CERN-ACC-2014-0159, 2014.
[8] A. Hofmann and B. Zotter, issued by ISR-TH-AH-BZ-amb, 1975, http://cds.cern.ch/record/1131122.
[9] J. Borer, A. Hofmann, J.-P. Koutchouk, T. Risselada, and B. W. Zotter, IEEE Trans. Nucl. Sci. **30**, 2406 (1983).
[10] J. E. Poole, in Proceedings of the third LEP performance workshop, SL Divisional Reports, 1993.
[11] I. Barnett, A. Beuret, P. Galbraith, K. N. Henrichsen, M. Jonker, G. Morpurgo, M. Placidi, R. Schmidt, L. Vos, J. Wenninger, I. Reichel, and F. A. Tecker, Dynamic beam based calibration of orbit monitors at LEP, revised version, Technical Report No. CERN-SL-95-97-BI, 1995.
[12] G. H. Hoffsttter, HERA accelerator studies 2000, Technical Report No. DESY-HERA-2000-07, 2000.
[13] A. Jansson, P. Lebrun, and J. T. Volk, in *Proceedings of the 21st Particle Accelerator Conference, Knoxville, TN, 2005* (IEEE, Piscataway, NJ, 2005), p. 2272.
[14] Z. Martí, J. Campmany, X. N. Gavaldà, J. Marcos, and V. Massana, in Proceedings of 6th International Particle Accelerator Conference, Richmond, VA, USA (2015), pp. 338–340.
[15] J. Kewisch, S. Peggs, T. Satogata, G. Goddere, S. Tepikian, and D. Trbojevic, in *Proceedings of the 6th European Particle Accelerator Conference, Stockholm, 1998* (IOP, London, 1998), p. 1620.
[16] L. Ahrens, M. Bai, V. Ptitsyn, T. Satogata, D. Trbojevic, and J. van Zeijts, in *Proceedings of the Particle Accelerator Conference, Chicago, IL, 2001* (IEEE, New York, 2001), pp. 3135–3137.

[17] M. G. Minty and F. Zimmermann, *Measurement and Control of Charged Particle Beams, Particle Acceleration and Detection* (Springer, Berlin, 2003).
[18] W. Scandale, Revisiting the problem of the LHC insertion symmetry, Technical Report No. SL-Note-94-42-AP, 1994.
[19] F. A. Golfe, Looking for a symmetric LHC low-beta insertion, Technical Report Nos. SL-Note-95-70-AP, LHC-NOTE-336, 1995.
[20] MAD-X: Methodical accelerator design, http://madx.web.cern.ch/madx/.
[21] J. Bengtsson and J. Irwin, Analytical calculations of smear and tune shift, Technical Report No. SSC-232, 1990.
[22] J. Coello de Portugal, F. Carlier, A. Garcia-Tabares, A. Langner, E. Maclean, L. Malina, M. McAteer, T. Persson, P. Skowroski, and R. Tomás, in *Proceedings of the International Particle Accelerator Conference No. 7, IPAC 16* (JACoW, Busan, 2016), p. 3480.
[23] S. Y. Lee, *Accelerator Physics*, 3rd ed. (World Scientific, Singapore, 2012).
[24] H. Wiedemann, *Particle Accelerator Physics*, 3rd ed. (Springer, Berlin, 2007).
[25] H. A. Enge, Rev. Sci. Instrum. **35**, 278 (1964).
[26] MQXF Collaboration Workspace, https://espace.cern.ch/HiLumi/WP3/SitePages/MQXF.aspx.
[27] S. Kelly, M. Thomas, R. Appleby, L. Thompson, B. Holzer, R. de Maria, and S. Russenschuck, Study of the impact of fringe fields of the large aperture triplets on the linear optics of the HL-LHC, Technical Report No. CERN-ACC-2013-0174, 2013.
[28] M. Fitterer, Follow-up of powering schemes for it, q4 and d1/d2, HL-LHC TC meeting, 2015.
[29] M. Fitterer, Powering schemes for inner triplet, q4 and d1/d2, HL-LHC TC meeting, 2015.
[30] M. Kuhn, Status of wire-scanner and *k* modulation, LBOC meeting, 2015.
[31] J. Wenninger, W. Hofle, S. Redaelli, and M. Lamont, LHC status weekend, 2015, LHC morning meeting, 2015.
[32] M. Fitterer, S. Fartoukh, M. Giovannozzi, and R. De Maria, Report No. TUPTY036, 2015, p. 48.
[33] A. Garcia-Tabares Valdivieso, L. Malina, B. M. Salvachua Ferrando, P. K. Skowronski, M. Solfaroli Camillocci, R. Tomas Garcia, J. Wenninger, and J. M. Coello De Portugal Martinez Vazquez, MD test of a ballistic optics, Technical Report No. CERN-ACC-NOTE-2016-0008, 2016.
[34] P. Skowroski, F. Carlier, J. Coello de Portugal, A. Garcia-Tabares, A. Langner, E. Maclean, L. Malina, M. McAteer, T. Persson, and R. Tomás, in *Proceedings of the International Particle Accelerator Conference No. 7, IPAC 16, Geneva, Switzerland, 2016* (JACoW, Busan, 2016), p. 3343.
[35] E. H. Maclean, F. S. Carlier, S. Fartoukh, T. H. B. Persson, P. K. Skowronski, R. Tomas Garcia, and D. A. Wierichs, Report No. (2016).